

## BIMETALLIC AU/AG METAL SUPERSTRUCTURES FROM MACROMOLECULAR METAL COMPLEXES IN SOLID-STATE

CARLOS DIAZ<sup>a\*</sup>, MARIA LUISA VALENZUELA<sup>b</sup> AND DANIELA BOBADILLA<sup>a</sup>

<sup>a</sup>Departamento de Química, Facultad de Química, Universidad de Chile. Las Palmeras 3425, Nuñoa, casilla 653, Santiago de Chile, Chile.

<sup>b</sup>Universidad Andres Bello, Departamento de Ciencias Químicas, Facultad de Ciencias Exactas. Av. Republica 275, Santiago, Chile.

(Received: June 25, 2013 - Accepted: September 25, 2013)

### ABSTRACT

Novel bimetallic Au/Ag superstructures have been prepared from solid-state pyrolysis of the macromolecular complexes Chitosan(MLn/M'Ln)<sub>n</sub> y PSP-4-PVP×(MLn/M'Ln)<sub>n</sub> with MLn = AuCl<sub>3</sub> and M'Ln = Ag(CF<sub>3</sub>SO<sub>3</sub>). The characterization was made from XRD (X-ray diffraction of powder), SEM and EDS analysis. Morphologies are influenced by both the nature of the polymer and the metal/polymer, molar ratio of the polymer precursor. EDS analysis suggests a core/shell Au/Ag structure for the materials. A probable mechanism of the formation of these superstructures is discussed. Although separated reports of metallic superstructures of Au or Ag have been recently described, the here reported are the first bimetallic Au/Ag.

**Key words:** Superstructures, Macromolecular complexes, metallic Au and Ag, Pyrolysis

### INTRODUCTION

Noble metal structures usually can be obtained in both as bulk and/ or nanostructured materials<sup>1-3</sup>. However a third form, called 3D supracrystals or superlattices have recently emerged<sup>4-6</sup>. These can be obtained by destabilization of the Au solution nanoparticles, usually by elimination of the solvent. These materials have interesting collective intrinsic properties. The few reported preparation methods for this type of materials have been developed in solution and not solid-state approximation has been done. Thus, among the few reports on this type of materials no bimetallic Au/Ag superstructures have been reported, only Au or Ag superlattices<sup>4-6</sup>. Here we report a solid-state method to prepare Au/Ag superstructures from pyrolysis of the macromolecular precursors Chitosan(MLn/M'Ln)<sub>n</sub> y PSP-4-PVP×(MLn/M'Ln)<sub>n</sub> with MLn=AuCl<sub>3</sub> and M'Ln= AgCF<sub>3</sub>SO<sub>3</sub>, PSP-4-PVP = poly[styrene-block-(4-vinylpyridine)].

We have previously reported a solid-state method to prepare metallic and/ or metal oxides nanostructured materials (see Figure 1). Solid-state pyrolysis of organometallic derivatives of cyclic and/or polyphosphazenes at 800 °C affords metallic nanostructures of the type M<sub>x</sub>O<sub>y</sub> and M<sub>x</sub>P<sub>y</sub>O<sub>z</sub><sup>7-21</sup>.

However, due to the presence of phosphorus in the polymeric chain, the nanostructured materials usually involve phosphates and/or pyrophosphates metallic phases<sup>16</sup>. When the cyclic and/or polyphosphazenes have coordinated two organometallic fragments as CpFe(dppe)<sup>+</sup> and TIPF<sub>6</sub><sup>-</sup>, the bimetallic core/shell Fe<sub>2</sub>Fe<sub>3</sub>(P<sub>2</sub>O<sub>7</sub>)<sub>4</sub>/Ti<sub>3</sub>P<sub>3</sub>O<sub>9</sub> nanoparticles are obtained<sup>21</sup> after pyrolysis. Therefore, if we want to obtain pure bimetallic nanoparticles, a polymer not containing phosphorus within the polymeric chain could be desirable. It is expected that phosphorus-less organic polymers have the potential to be good solid-state templates of metallic and organometallic-macromolecular complexes during their pyrolysis. We have selected Chitosan and PSP-4-PVP due to their ability to coordinate ion metals through the nitrogen atoms to form macromolecular metal-polymer complexes precursors<sup>22-29</sup>.

### EXPERIMENTAL

AuCl<sub>3</sub> and Ag(CF<sub>3</sub>SO<sub>3</sub>), PSP-co-4-PVP and Chitosan were purchase from Aldrich and used as received. All the reactions were performed in CH<sub>2</sub>Cl<sub>2</sub> as solvent and reaction time was one week.

#### Precursors Synthesis

##### General Procedure Chitosan(MLn/M'Ln)<sub>n</sub>

In a typical synthesis, the respective metallic salts, AuCl<sub>3</sub> and Ag(CF<sub>3</sub>SO<sub>3</sub>) were added in a Schlenk tube over the CH<sub>2</sub>Cl<sub>2</sub> solvent under magnetic stirring and then the respective Chitosan amount according the 1:1, 1:5 or molar ratio. Reaction time and other details for each metallic salts reaction are given in Table 1. After this the supernatant solution (if the solid decanted) was extracted with a syringe and the solid dried under reduced pressure to give a yellow-red solid (Table 1). Owing to their insolubility characterization of the precursors

was made only by elemental analysis and IR spectroscopy. Coordination was confirmed by the behavior of the broad ν(OH) in Chitosan<sup>20</sup> which becomes unfolded upon coordination, and exhibiting a new band around 3100 cm<sup>-1</sup>. PSP-co-4-PVP coordination was evidenced by the appearance of a characteristic band in the range 1600-1650 cm<sup>-1</sup> corresponding to coordinate pyridine<sup>10,20</sup>.

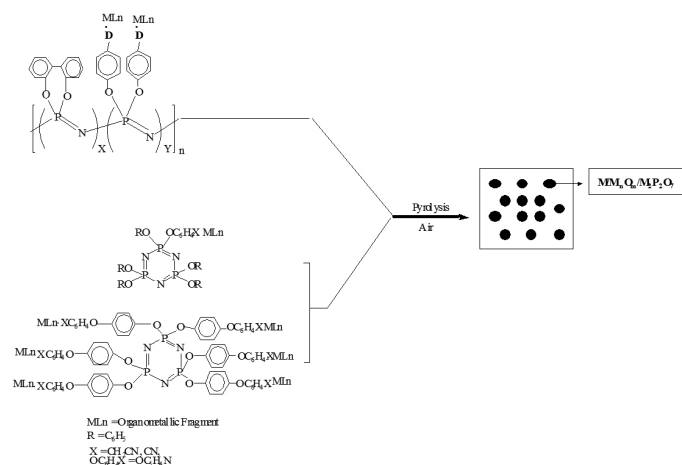


**Figure 1** Schematic representation of the solid-state method to obtain nanostructured materials from oligomeric and polymeric precursors.

##### General Procedure PSP-4-PVP/(MLn/M'Ln)<sub>n</sub>

In a typical synthesis the respective metallic salt AuCl<sub>3</sub> and Ag(CF<sub>3</sub>SO<sub>3</sub>) were added in a Schlenk tube over the CH<sub>2</sub>Cl<sub>2</sub> solvent under magnetic stirring and then the respective Poly(styrene-co-4-vinylpyridine) amount according to the 1:1 or 1:5 molar ratio. After approximate 6 days the supernatant solution (provided the solid decanted) was extracted with a syringe and the solid dried under reduced pressure to give a solid with diverse colors. In some cases the polymer undergoes an extensive gel formation. In such case the solvent was eliminated at reduced pressure using a high vacuum pump and/or using a furnace with vacuum. PSP-co-4-PVP coordination was evidenced by the appearance of a characteristic band in the range 1600-1650 cm<sup>-1</sup> corresponding to coordinate pyridine<sup>10,20</sup>.

Elemental analyses (%): **(1)** C, 10.93; H, 1.71; N, 1.8; S, 3.91. **(2)** C, 24.12; H, 3.88; N, 4.70; S 3.37. **(3)** C, 7.3; H, 0.74; N, 1.08; S, 1.22. **(4)** C, 38.74; H, 3.2; N, 5.9; S, 3.59. Owing the complex and uncertain exact formula of the precursor, the calculated C, H and N content was not possible to estimate.

**Table 1.** Experimental details of the precursors formation<sup>a</sup>

No	Precursor	Ratio <sup>b</sup>	Polymer(g)	Au(g) <sup>c</sup>	Ag(g) <sup>d</sup>	Color of the product
1	Chitosan(MLn/M <sup>l</sup> Ln) <sub>n</sub>	1:1	0.225	0.4	0.34	Bright brown-yellow
2	Chitosan(MLn/M <sup>l</sup> Ln) <sub>n</sub>	1:5	1.16	0.4	0.34	Bright brown-yellow
3	PSP-4-PVP×(MLn/M <sup>l</sup> Ln) <sub>n</sub>	1:1	0.145	0.4	0.35	Bright yellow
4	PSP-4-PVP×(MLn/M <sup>l</sup> Ln) <sub>n</sub>	1:5	0.698	0.4	0.34	Bright yellow

<sup>a</sup> In all the reactions a solvent volume of 40 mL was used.

<sup>b</sup> Polymer/metal relation

<sup>c</sup> AuCl<sub>3</sub>

<sup>d</sup> Ag(CF<sub>3</sub>SO<sub>3</sub>)

### Pyrolysis

The pyrolysis experiments were conducted by pouring a weighed portion (0.05–0.15 g) of the respective precursor into aluminum oxide boats that were placed in a furnace (Labtech LEF-10 oven) under a flow of air, heating from 25 °C to upper temperature limits of 300 °C, and then to 800 °C, followed by annealing for 2–4 h and at rates of 10 °C min<sup>-1</sup> in each case.

### Characterization of the pyrolytic products

Solid pyrolytic samples were characterized by X-Ray diffraction of powders (XRD) and scanning electron microscopy (SEM). SEM images were acquired with a JSM-6380LV, Jeol Ltda. microscope, with an acceleration potential of 20 keV. Energy dispersive X-ray analysis (EDAX) was performed on a NORAN Instrument micro-probe attached to a JEOL 5410 scanning electron microscope. X-ray diffraction (XRD) was conducted at room temperature on a Siemens D-5000 diffractometer with  $\theta$ -2 $\theta$  geometry. The XRD data was collected using Cu-K $\alpha$  radiation (40 kV, 30 mA). FTIR measurements were performed on a Perkin Elmer FTIR spectrophotometer model Spectrum BXII using KBr pellets. Elemental analysis were performed on a FISON'S INSTRUMENTS, model EA 1108 CHNS-O instruments (Pontificia Universidad Catolica de Chile)

## RESULTS AND DISCUSSION

Figure 2 shows the XRD patterns of the pyrolytic products from the precursors Chitosan(AuCl<sub>3</sub>/Ag(CF<sub>3</sub>SO<sub>3</sub>)<sub>n</sub>) and PSP-4-PVP×(AuCl<sub>3</sub>/Ag(CF<sub>3</sub>SO<sub>3</sub>)<sub>n</sub>) precursors with molar ratios 1:1. The lattice constants for Au and Ag are very similar so their XRD are totally overlapped preventing discrimination of Au-Ag bimetallic phase from either monometallic phase based on the XRD patterns<sup>30-32</sup>. Therefore the presence of core/shell or alloys Au/Ag structures can be distinguished by TEM imaging<sup>33,34</sup> or by Uv-visible spectroscopy<sup>35-37</sup>. The presence of Au and Ag can be confirmed by EDS analyses<sup>32</sup>.

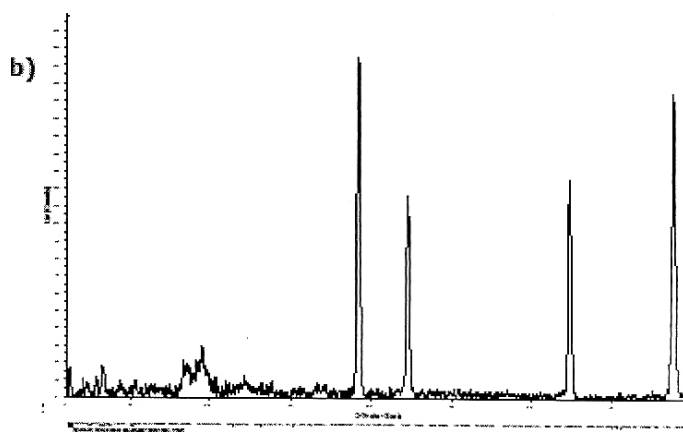
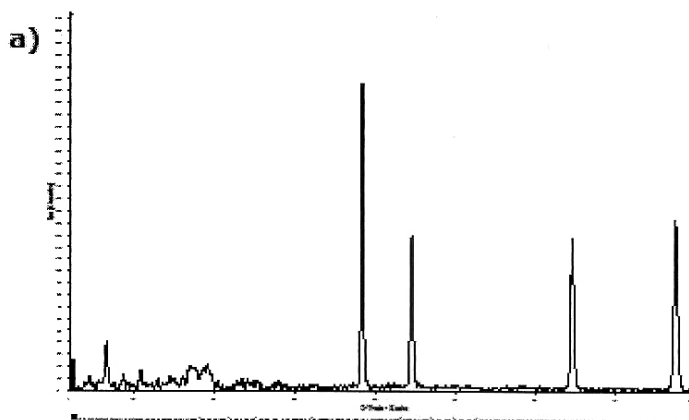


**Figure 2.** XRD patterns of pyrolytic products from Chitosano(AuCl<sub>3</sub>/Ag(CF<sub>3</sub>SO<sub>3</sub>)<sub>n</sub>) a) and PSP-4-PVP×(AuCl<sub>3</sub>/Ag(CF<sub>3</sub>SO<sub>3</sub>)<sub>n</sub>) b), both with molar ratio 1:1.

Using this technique is normally possible only when the Au/Ag nanoparticles are prepared in solution.

In our case the characterization using these two techniques is not possible because the pyrolytic products are very hard solid materials and they cannot be ground or cut into thin films for to be mounted on the grid of the TEM apparatus or be mounted as a powder in the UV-visible reflectance diffuse holder. However by SEM-EDS analysis<sup>32</sup> a possible structure of Au/Ag bimetallic materials can be proposed. Figure 3 shows the SEM image of the pyrolytic products from all precursors. As can be viewed from Figure 3 the morphology of the product depends on both the nature of the polymer (ie compare Figure 3a with 3b and 3c with 3d) and on the ratio formation of the precursor (ie compare Figure 3a with 3c and 3b with 3d). For a constant molar ratio metal/polymer ie. 1:1 the PSP-4-PVP induces most porous materials than Chitosan. On the other hand for a constant polymer (PSP-4-PVP or Chitosan), the 1:1 metal/polymer ratio induces a most dense material than with a 1:5 ratio.

This can be due to the most near linked Au and Ag centers in the polymeric chain in the 1:1 ratio of the both polymeric precursors. However these conclusions could be valid, although the Figure 3d was taken in a greater magnification.

The presence of gold and silver in the pyrolytic materials was confirmed by EDS analysis. As shown in Figure 4a,b for the pyrolytic products from 1:1 PSP-4-PVP×(AuCl<sub>3</sub>/Ag(CF<sub>3</sub>SO<sub>3</sub>)<sub>n</sub>) and 1:1 Chitosan(AuCl<sub>3</sub>/Ag(CF<sub>3</sub>SO<sub>3</sub>)<sub>n</sub>) precursors, the presence of gold and silver is evident. For the other pyrolytic product similar SEM/EDS images were observed. The nature of the Au/Ag bimetallic materials become clear by observing the quantitative ESD analysis where an approximate content Au/Ag of 2:1 characteristic of core/shell<sup>38,39</sup> was observed see Figure 5. A possible representation of these are given in Figure 6.

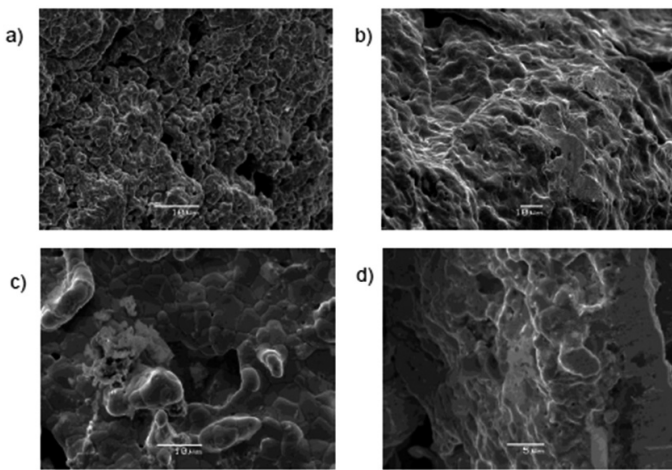


**Figure 3** SEM images of the pyrolytic products from precursors : a) PSP-4-PVP•(AuCl<sub>3</sub>/Ag(CF<sub>3</sub>SO<sub>3</sub>))<sub>n</sub> 1:1 ; b) Chitosan•AuCl<sub>3</sub>/Ag(CF<sub>3</sub>SO<sub>3</sub>))<sub>n</sub> 1:1 ; c) PSP-4-PVP•(AuCl<sub>3</sub>/Ag(CF<sub>3</sub>SO<sub>3</sub>))<sub>n</sub> 1:5 d) Chitosan•AuCl<sub>3</sub>/Ag(CF<sub>3</sub>SO<sub>3</sub>))<sub>n</sub> 1:5

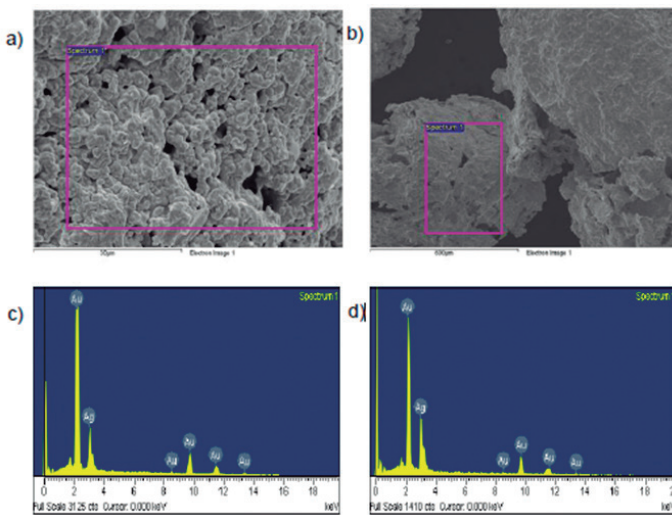


**Figure 4** a) SEM image and their c) EDS analysis for the pyrolytic product from 1:1 from 1:1 PSP-4-PVP•(AuCl<sub>3</sub>/Ag(CF<sub>3</sub>SO<sub>3</sub>))<sub>n</sub> precursor (a,c) and for 1:1 Chitosano•(AuCl<sub>3</sub>/Ag(CF<sub>3</sub>SO<sub>3</sub>))<sub>n</sub> (b, d) .

A linear EDS scanning for a line through a zone of the pyrolytic product from 1:1 PSP-4-PVP•(AuCl<sub>3</sub>/Ag(CF<sub>3</sub>SO<sub>3</sub>))<sub>n</sub> precursor is shown in Figure 5. It can be observed a double content of the Au in relation to the Ag content which could be indicative of a core/shell structure<sup>38</sup>, see Figure 6. The junction of these core/shell nanoparticles in a 3D manner would give rise to the observed “superstructures” by SEM.

Monolithic nanoporous gold structures are interesting materials with unusual application and peculiar properties such as mechanical strength and stiffness<sup>40,41</sup>. Recently it was reported that Au disks of nanoporous morphology exhibit a 10<sup>8</sup> factor surface enhanced Raman scattering<sup>42</sup>. The Au/Ag bimetallic materials reported here could then have some

SERS (Surface-enhanced Raman scattering) activity which could be enhanced in relation to Au and Ag individual due to some cooperative bimetallic effect.

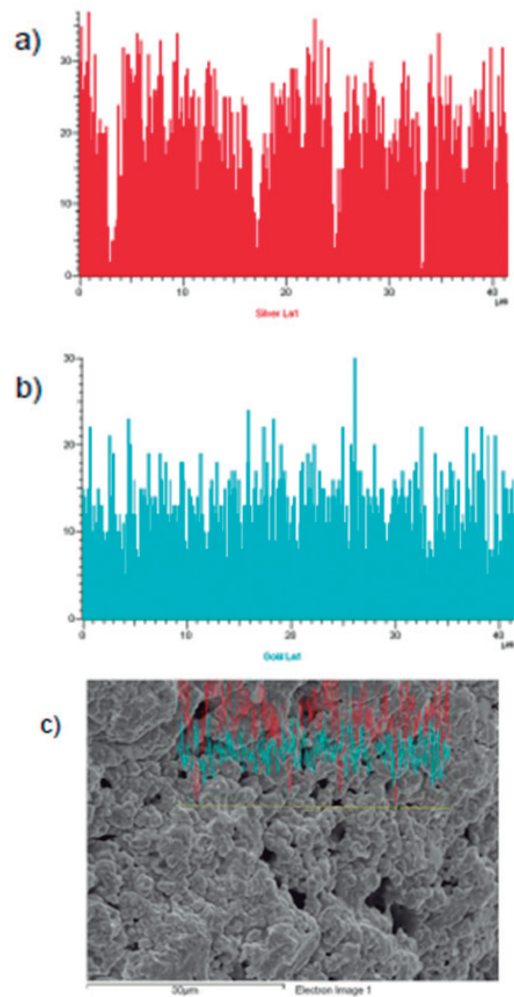


**Figure 5.** Au a) and Ag b) profile content for the pyrolytic product from PSP-4-PVP•(AuCl<sub>3</sub>/Ag(CF<sub>3</sub>SO<sub>3</sub>))<sub>n</sub> 1:1 precursor in the line marked by yellow line in c).

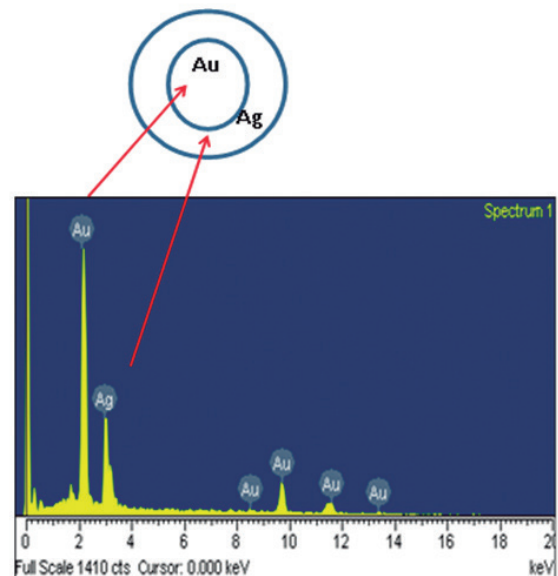


**Figure 6.** Representative structure of the Core/shell Au/Ag nanoparticles



### Probable mechanism formation

The most likely mechanism for the formation of the Au/Ag superstructures may be similar to mechanisms that have been previously established as general for the solid-state pyrolysis of metallic and organometallic derivatives cyclic-oligomer-phosphazene and polyphosphazene<sup>7-21</sup>. Figure 7 shows a schematic representation of the probable formation mechanism of the pyrolytic product.

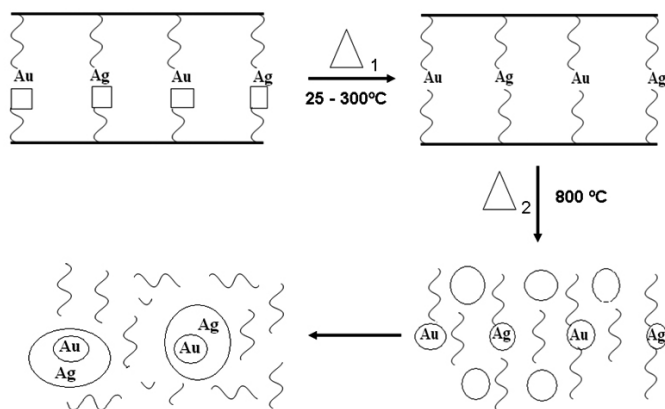


**Figure 7.** schematic representation of the probable formation mechanism of the pyrolytic products.

The first step involves the cross-linking<sup>13</sup> of the polymer induced by the coordination by the PSP-co-4-PVP or Chitosan polymer chains to the metal centers during the initial annealing step, followed by the carbonization of the organic matter to produce holes where the metal centers begin to coarsen and grow<sup>43</sup>. Carbonization of the organic matter usually occurs during pyrolysis of metallic and organometallic derivatives of polymers around 350 °C<sup>43</sup>. Some incomplete combustion always produces some CO<sup>44</sup> which reduces the metallic Au(I) and Ag(I) salts to Au and Ag which bind together. Subsequently join of these core/shell nanoparticles produce the 3D “superstructures”.

Also in the combustion process a sudden loss of nitrogen –arises from the pyridine groups of PSP-co-4-PVP or NH<sub>2</sub> Chitosan- induces foamy materials<sup>44</sup>.

### CONCLUSIONS

The first solid-state method to prepare Au/Ag superstructures is reported. Chitosan(MLn/M’Ln)<sub>n</sub> and PSP-4-PVP×(MLn/M’Ln)<sub>n</sub> with MLn = AuCl<sub>3</sub> and M’Ln = Ag(CF<sub>3</sub>SO<sub>3</sub>) are convenient precursors to superlattices Au/Ag materials. The morphology of the “foams like” products depends both on the nature of the polymer as well as to the molar ratio polymer/metallic salt. The polymer PSP-4-PVP and the ratio 1.1 induce the most porous morphologies. The probable mechanism involves the formation of a cross-linking matrix with subsequent combustion of the organic matter where the bimetallic foams grow.

### ACKNOWLEDGMENTS

To Fondecyt No 1120179 for financial support.

### REFERENCES

- R. Sardar, A.M. Funston, P. Mulvaney and R.W. Murray *Langmuir*, **25**, 138, (2009).
- G. Schmid and B. Corain *Eur. J. Inorg. Chem.* 3081, (2003).
- M. Ch. Daniel and D. Astruc *Chem. Rev.* **104**, 293, (2004).
- Y.F. Wan, N. Goubet, P.A. Albouy and M.P. Pileni *Langmuir* DOI: dx.doi.org/10.1021/la3045187
- M. P. Pileni *Acc. Chem. Res.* **40**, 685, (2007).
- M.P. Pileni *J. Chem. Mater.* **21**, 16748, (2011).
- C. Díaz and M. L. Valenzuela *J. Chil. Chem. Soc.* **50**, 417, (2005).
- C. Díaz, P. Castillo and M. L. Valenzuela *J. Cluster. Science* **16**, 515, (2005).
- C. Díaz and M. L. Valenzuela, *J. Inorg. Organomet. Polym. Mater.* **16**, 123, (2006).
- C. Díaz and M. L. Valenzuela *Macromolecules* **39**, 103, (2006).
- C. Díaz and M. L. Valenzuela *J. Inorg. Organomet. Polym. Mater.* **16**, 211, (2006).
- C. Díaz and M. L. Valenzuela *J. Inorg. Organomet. Polym. Mater.* **16**, 419, (2006).
- C. Díaz, M. L. Valenzuela, L. Zuñiga, C. O’Dwyer, *J. Inorg. Organometallic. Polymer* **19**, 507, (2009).
- C. Díaz, M. L. Valenzuela, D. Bravo, V. Lavayen and C. O’Dwyer *Inorg. Chem.* **47**, 11561, (2008).
- C. Díaz, M. L. Valenzuela, E. Spodine, Y. Moreno and O. Peña *J. Cluster Science* **18**, 831, (2007).
- J. Jimenez, A. Laguna, M. Benouazzane, J. A. Sanz, C. Díaz, M. L. Valenzuela, P. G. Jones *Chem. Eur. J.* **15**, 13509, (2009).
- C. Díaz, M. L. Valenzuela, A. Laguna, V. Lavayen, J. Jimenez, L. Power and C. O’Dwyer *Langmuir* **26**, 10223, (2010).
- C. Díaz, V. Lavayen, and C. O’Dwyer *J. Solid State Chemistry* **183**, 1595, (2010).
- C. Díaz, M. L. Valenzuela, D. Bravo, C. Dickinson and C. O’Dwyer *Journal of Colloids and Interface Science* **362**, 21, (2011).
- C. Díaz, M. L. Valenzuela, V. Lavayen, K. Mendoza, O. Peña, C. O’Dwyer *Inorganica Chimica Acta* **377**, 5, (2011).
- C. Díaz, M. L. Valenzuela and N. Yutronic *Journal of Inorganic and Organometallic Polymers* **17**, 577, (2007).
- K. Ogawa and K. Oka *Chem. Mater.* **5**, 726, (1993).
- S. Schlick *Macromolecules* **19**, 192, (1986).
- R. Hernandez, O. Reyes and A.R. Rumlho *J. Braz. Chem. Soc.* **18**, 1388., (2007).
- P. Guo, W. Wenyan, G. Liang and P. Yao *J. Colloid. Interf. Sci.* **323**, 229, (2008).
- L. A. Belfiore, M. Pat Curdie and E. Ueda *Macromolecules* **26**, 6908, (1993).
- A. Haynes, P. M. Maitlis, R. Quyoum, C. Pulling, H. Adams, S. E. Spey, and R. W. Strange *J. Chem. Soc. Dalton Trans.* 2565, (2002).
- C. V. Franco, M. M. da SilvaPaula, G. Goulart, L. F. De Lima, L. K. Noda and N. S. Goncalves *Mater. Letters* **60**, 2549, (2006).
- M. Antonietti, E. Wenz, L. Bronstein and M. Seregina *Adv. Mater.* **7**, 1000, (1995).
- M. Tsuji, R. Matsuo, P. Jiang, N. Miyamae, D. Ueyama, M. Nishio, S. Hikino, H. Kumagai, K. Sozana and X. L. Tang *Crystal Growth and Design* **8**, 2528, (2008).
- X. Liu, A. Wang, X. Yang, T. Zhang, Ch.Y. Mou, D. Sh. Su and J. Li *Chem. Mater.* **21**, 410, (2009).
- Sh. Tokonami, N. Morita, K. Takasaki and N. Toshima *J. Phys. Chem. C.* **114**, 10336, (2010).
- T. Shibata, B.A. Bunker, Z. Zhang, D. Meisel, Ch. F. Vardeman II and J. D. Gezelter *J. Am. Chem. Soc.* **124**, 11989, (2002).
- J. H. Hodak, A. Henglein, M. Giersig and G.V. Hartland *J. Phys. Chem. B* **104**, 11708-11718, (2000).
- L. M. Liz-Marzan and A. P. Philipse *J. Phys. Chem.* **99**, 15120-15128, (1995).
- A. V. Singh, B. M. Bandgar, M. Kasture, B. L. Prasad and M. Sastry *J. Mater. Chem.* **15**, 5115, (2005).
- O. M. Wilson, R. W. J. Scott, J. C. Garcia-Martinez and R. M. Crooks *J. Am. Chem. Soc.* **127**, 1015-1024, (2005).
- S. Anandan, F. Grieser and M. Ashokkumar Toshima *J. Phys. Chem. C.* **112**, 15102, (2008).
- J. He, I. Ichinose, T. Kunitake, A. Nakao, Y. Shiraiishi and N. Toshima *J. Am. Chem. Soc.* **125**, 11034, (2003).
- J. Biener, A. Wittstock, L. A. Zepeda-Ruiz, M. M. Biener, V. Zielasek, D. Kramer, R. N. Viswanath, J. K. Weissmuller, M. Baumer, A. V. Hamza *Nature Materials* **28**, 47, (2009).
- L. Lefebvre, J. Banhart, D. Dunand Porous Metals and metallic Foams: Current status and recent Developments. *Advanced Engineering Materials* **10**, 775, (2008).
- J. Q. Pratik Motwani, M. Gheewala, Ch. Brennan, J. C. Wolfe and W. Ch. Shih *Nanoscale* **5**, 4105, (2013).
- C. Díaz, M.L. Valenzuela, V. Lavayen, and O’Dwyer *Inorganic Chemistry* **51**, 6228 (2012)
- B. Tappan, M.H. Huynh, M. A. Hiskey, D.E. Chavez, E.P. Luther, J.T. Mang and S.F. Son. *J Am Chem Soc* **128**, 6589, (2006).